Proceedings of the
44th IEEE Conference on Decision and Control, and
the European Control Conference 2005
Seville, Spain, December 12-15, 2005

H_∞ Loop Shaping Controller for Shape Memory Alloy Actuators*

J.Jayender R.V.Patel
Department of Electrical and Computer Engineering
University of Western Ontario
London, ON N6A 5B9, Canada
jjagadee@uwo.ca, rajni@eng.uwo.ca

S.Nikumb M.Ostojic
National Research Council of Canada
Integrated Manufacturing Technologies Institute
London, ON N6G 4X8, Canada
suwas.nikumb@nrc.gc.ca, mile.ostojic@nrc.gc.ca

***Abstract*— This paper describes a Robust H_∞ Controller for a Shape Memory Alloy actuator. A formulation based on concepts from physics, has been used to model the Shape Memory Alloy (SMA). The modelling equations include Joules heating - convectional cooling to explain the dynamics of temperature, Fermi-Dirac statistics to explain the variation of mole fraction with temperature, and a stress-strain constitutive equation to relate changes in mole fraction and temperature to changes in stress and strain of the SMA. An H_∞ loop shaping controller using normalized coprime stabilization is designed such that the gains are high when the model describes the SMA accurately and low at higher frequencies when the model is inaccurate. Simulation and experimental results show fast and accurate control of the strain in the SMA actuator.**

***Index Terms*— Shape Memory Alloy, Fermi-Dirac principle, robust loop-shaping H-infinity controller**

I. Introduction

In the last decade, there have been a few papers on modelling and control of Shape Memory Alloy (SMA) actuators. Most papers use a curve-fitting based method to develop a mathematical description of the SMA and use the dynamic equations thus obtained to control it. A continuous-time model, developed by Arai et. al. [4], fits a differential equation to experimental data. The model, however, does not guarantee a correct response over the entire operating region and is also not based on the physics of the process.

Some papers, e.g., see [5],[6],[9], have used the Preisach model to model the hysteresis nature of the SMA. Though, they are able to model the hysteresis characteristic of the SMA and the minor loops in the hysteresis graph, the formulation is not convenient for developing a control strategy.

Conventional PID control does not work well since the SMA demonstrates a nonlinear behaviour. Feedback linearization has been used to varying degrees of success [10],[11]. The problem with feedback linearization is that it depends on accurate cancellation of the nonlinear components of the SMA response which in turn depends on a large number of parameters. In order to overcome these problems, variable structure control has been utilized since the control strategy is fairly insensitive to uncertainties in the parameters of the model [7],[8]. However, the problem with variable structure control is that tracking is possible so long as the error is small. The discontinuous nature of switching also may introduce ringing and high frequency components in the system which are not desirable.

Most formulations for SMA are obtained by fitting mathematical models to experimental data. However, for biomedical applications, the actuator works in body fluids like blood. The model is no longer valid since the behaviour of the SMA actuator completely varies inside the body. In our previous paper [3], we developed a model for the SMA based on the laws of physics. In order to model the phase transformation from Martensite to Austenite and vice versa, we used the Fermi-Dirac principle from statistical physics to model the dynamics of the transformation. Modelling equations for the temperature dynamics and the constitutive equations have been used previously [7]. A gain-scheduled LQR optimization based PI controller was developed. Excellent simulation and experimental results were obtained. The LQR based controller also has the in-built property of rejecting uncertainties in the parameters of the model since it has a guaranteed stability margin. The problem however arises with unmodelled dynamics at high frequencies which may cause instability [12].

In this paper, we use the same model developed in [3]. A robust H_∞ loop-shaping controller has been developed to obtain a performance/robust stability tradeoff. The desired open-loop transfer function is chosen so that the gains are low at high frequencies where the unmodelled dynamics dominate.

II. Theory and Modelling

Shape memory alloys demonstrate a change in strain by a change in temperature due to a phase transformation from the Martensite phase to the Austenite phase and vice versa. The SMA in the Martensite phase is soft and can be easily deformed and exists at a lower temperature. However, on heating by means of electric current (Joule's heating) or by hot water, the SMA changes its phase from Martensite to Austenite. The arrangement of the atoms in the Austenite phase is more structured, making it harder and stronger than the Martensite phase.

A. *Modelling of Phase Transformation*

The Fermi-Dirac statistics has been used to describe the distribution of the SMA in the Austenite and Martensite

*This research was supported by the Natural Sciences and Engineering Research Council (NSERC) of Canada under grant RGPIN-1345 and by an infrastructure grant from the Canada Foundation for Innovation.

0-7803-9568-9/05/$20.00 ©2005 IEEE

phase, considering the SMA as a two-state system. Two modelling equations have been used based on whether the alloy is being heated or cooled due to hysteresis with two different transition temperatures. The phase transformation equation from Martensite to Austenite during heating is described by analogy with the Fermi-Dirac statistics in the form:

$$\xi = \frac{\xi_m}{1 + exp(\frac{T_{f_a} - T}{\sigma_a} + K_a\sigma)} \tag{1}$$

where ξ is the fraction of the Austenite phase, ξ_m is the fraction of the Martensite phase prior to the present transformation from Martensite to Austenite, T is the temperature, T_{f_a} is the transition temperature from Martensite to Austenite, σ_a is an indication of the range of temperature around the transition temperature T_{f_a} during which the phase change occurs, σ is the stress and K_a is the stress curve-fitting parameter which is obtained from the loading plateau of the stress-strain characteristic with no change in temperature.

On cooling, the Austenite phase gets converted to the Martensite phase and the modelling equation during cooling is described by analogy with the Fermi-Dirac statistics in the form:

$$\xi = \frac{\xi_a}{1 + exp(\frac{T_{f_m} - T}{\sigma_m} + K_m\sigma)} \tag{2}$$

where ξ_a is the fraction of the Austenite phase prior to the present transformation from Austenite to Martensite, T is the temperature, T_{f_m} is the transition temperature from Austenite to Martensite, σ_m is an indication of the range of temperature around the transition temperature T_{f_m} during which the phase change occurs, σ is the stress and K_m is the stress curve-fitting parameter which is obtained from the unloading part of the stress-strain characteristic.
Since the SMA is modelled as a two-component system, at any given time, the sum of the mole fractions of the Austenite and Martensite phase is 1, i.e.,

$$\xi_a + \xi_m = 1 \tag{3}$$

The time derivatives of Eqns.(1) and (2) are as follows:
For heating:

$$\dot{\xi} = \frac{\xi^2}{\xi_m}[exp(\frac{T_{f_a} - T}{\sigma_a} + K_a\sigma)][\frac{\dot{T}}{\sigma_a} - K_a\dot{\sigma}] \tag{4}$$

For cooling:

$$\dot{\xi} = \frac{\xi^2}{\xi_a}[exp(\frac{T_{f_m} - T}{\sigma_m} + K_m\sigma)][\frac{\dot{T}}{\sigma_m} - K_m\dot{\sigma}] \tag{5}$$

The above equations model the phase transformations at the microscopic level and therefore accurately describe the behaviour of the SMA.

B. *Modelling of Temperature Dynamics*

The SMA actuator is heated by the process of Joules heating by applying a voltage across the SMA. The loss of heat from the SMA is through natural convection. Mathematically, the dynamics of the temperature are given by equation (6) and have also been used in [7].

$$\dot{T} = \frac{1}{mc_p}[\frac{V^2}{R} - hA(T - T_a)] \tag{6}$$

where m is the mass per unit length, c_p is the specific heat capacity, V is the voltage applied across the SMA, R is the resistance per unit length, h is the coefficient of convection, $A = \pi d$ is the circumferential area of cooling, d is the diameter of the wire, T is the temperature and T_a is the ambient temperature. The coefficient h is assumed to have the characteristics of a second-order polynomial to enhance the rate of convection at higher temperatures as observed in open-loop results:

$$h = h_0 + h_2T^2 \tag{7}$$

C. *Constitutive Equation*

The constitutive equation relating changes in stress, strain, temperature and mole fraction is given by the following equation and has been previously used in [7].

$$\dot{\sigma} = D\dot{\epsilon} + \theta_t\dot{T} + \Omega\dot{\xi} \tag{8}$$

where σ is the stress in the SMA, D is the average of Young's Moduli for the Martensite and Austenite phases, ϵ is the strain, θ_t is the thermal expansion factor and $\Omega = -D\epsilon_0$ is the phase transformation contribution factor. The model explains the hysteresis as well as the minor loops in the hysteresis, as illustrated in Figure 1.

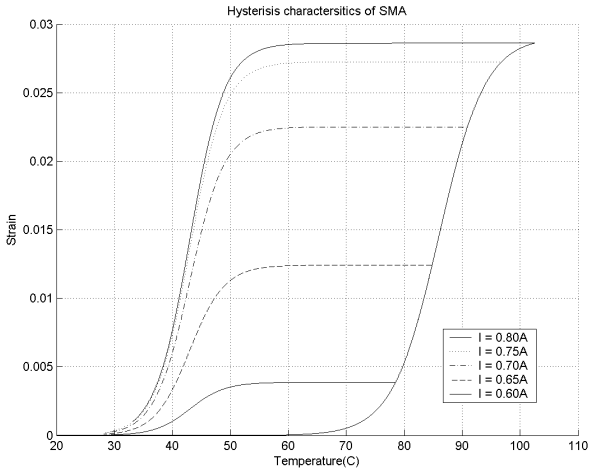

Fig. 1. Hysteresis Characteristics of SMA for varying sinusoidal input

III. Experimental Setup

In the experimental setup, the SMA wire is attached between a fixed support and a motor which provides a constant tension to keep the wire taut at all times. The readings from the encoder of the motor give the change in strain in the SMA wire which is fed to a computer through an encoder card. The real-time implementation of the gain-scheduled robust controller was done in C++ on a Windows

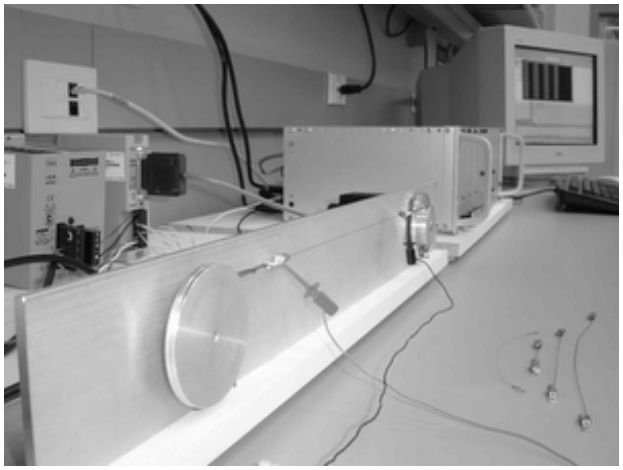

Fig. 2. Experimental setup

based PC at a sampling rate of about 100Hz. The setup is shown in Figure 2.

IV. No-Load Simulation of the Model

No-load simulation was done in MATLAB for the SMA actuator based on the above modelling equations. Since no load was assumed, σ and $\dot{\sigma}$ are equal to zero. A sinusoidal input voltage V was applied to the SMA model and the resulting strain vs. temperature was plotted to demonstrate the hysteresis nature of SMA, as shown in Figure 1.

The simulation results were also matched with the experimental open-loop results for a sinusoidal input to obtain the parameters of the model. The parameters used for modelling the SMA are given in Table 1.

V. Robust Controller

The dynamic characteristics of the SMA are completely defined by equation (4) or (5) (heating or cooling), together with equations (6) and (8).

We can also define σ_e as the integral of the error, i.e.,

$$\dot{\sigma_e} = \epsilon - \epsilon_{ref} \tag{9}$$

where ϵ is the strain of the SMA actuator and ϵ_{ref} is the reference trajectory. The state-space representation of the dynamic equations of the SMA along with equation (9) is:

$$\dot{\bar{z}} = f(\bar{z}, u, t) \tag{10}$$

where

$$\bar{z} = \begin{bmatrix} \epsilon \\ T \\ \xi \\ \sigma_e \end{bmatrix}$$

and u is the input voltage to the SMA wire. The nonlinear equations are linearized about a set of operating points $(\epsilon_0, T_0, \xi_0, u_0)$ on the reference trajectory.

To obtain the operating points, ϵ_0 is chosen as the value of the reference strain at that instant of time. T_0 and ξ_0 are obtained by integrating equations (4) or (5) and (8), depending on whether the SMA is being heated or cooled, for a given value of ϵ_0. The value of u_0 is obtained from equation (6) for a given value of T_0, assuming steady-state conditions.

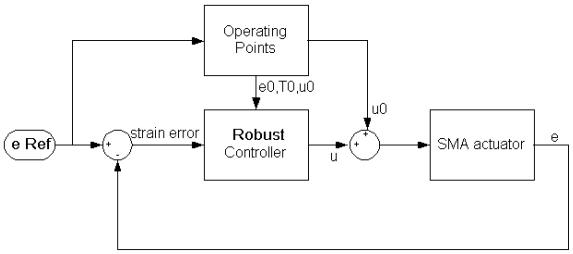

Fig. 3. Robust controller for the SMA actuator

Equation (10) is linearized about the calculated operating points to obtain linear models in the form

$$\dot{\bar{z}} = \mathbf{A}\bar{z} + \mathbf{B}u \tag{11}$$

$$y = \mathbf{C}\bar{z} \tag{12}$$

where

$$\mathbf{A} = \left[\frac{\partial f}{\partial \bar{z}}\right]_{\epsilon_0, T_0, \xi_0, u_0} \qquad \mathbf{B} = \left[\frac{\partial f}{\partial u}\right]_{\epsilon_0, T_0, \xi_0, u_0}$$

For the no-load case, which is the case considered here, σ and $\dot{\sigma}$ are equal to zero. In this case, the model given by (11) is not controllable since the number of independently controllable states is only 2. On removing the uncontrollable modes, the following state space model is obtained:

$$\dot{\bar{x}} = \mathbf{A}'\bar{x} + \mathbf{B}'u \tag{13}$$

where

$$\bar{x} = \begin{bmatrix} \epsilon \\ \sigma_e \end{bmatrix}$$

For a PI controller, the feedback is of the form

$$u = -K_P(\epsilon - \epsilon_{ref}) - K_I\sigma_e + u_0 \tag{14}$$

where K_P is the proportional gain and K_I is the integral gain. Writing $\mathbf{K} = \begin{bmatrix} K_p & K_I \end{bmatrix}$, the gains are computed by the loop-shaping procedure using normalized coprime stabilization [1],[2].

The nominal plant (SMA) is first shaped by using a precompensator W_1 so that the singular values of the nominal plant G are shaped to a desired open-loop shape. The compensator also ensures that the shaped plant $G_s = GW_1$ is square and G_s has no hidden modes.

For ensuring robust stabilization, ϵ_{max} is calculated as

$$\epsilon_{max} = \left(\inf_{K stabilizing} \left\| \begin{bmatrix} I \\ K \end{bmatrix} (I + G_s K)^{-1} \tilde{M}_s^{-1} \right\|_\infty \right)^{-1} \tag{15}$$

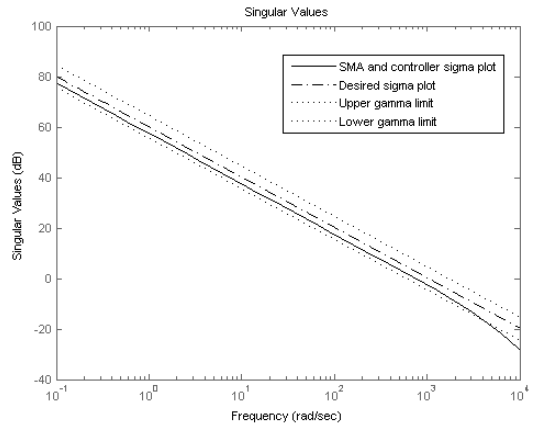

Fig. 4. Sigma plots of open-loop SMA and Controller transfer funtion

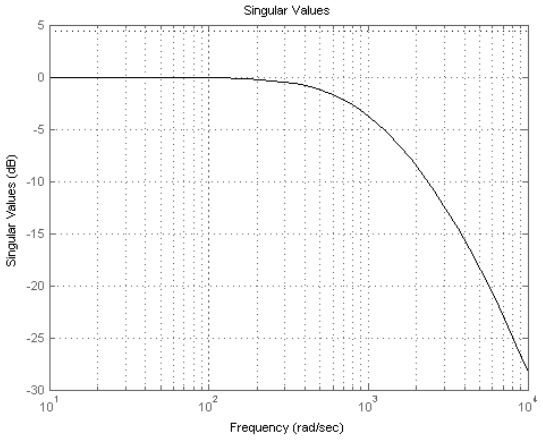

Fig. 5. Sigma plot of closed-loop SMA and Controller transfer funtion

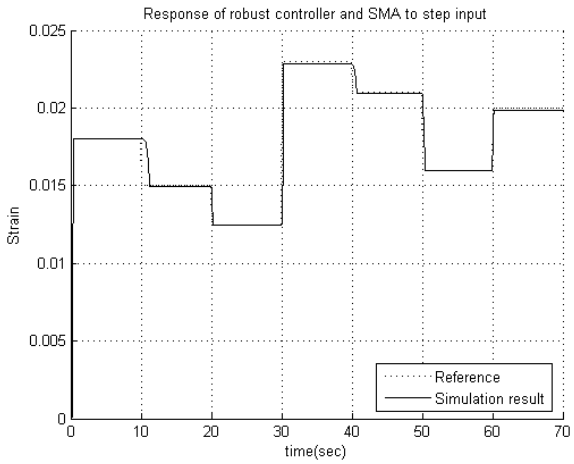

Fig. 6. Simulation result: Closed-loop SMA response to step changes

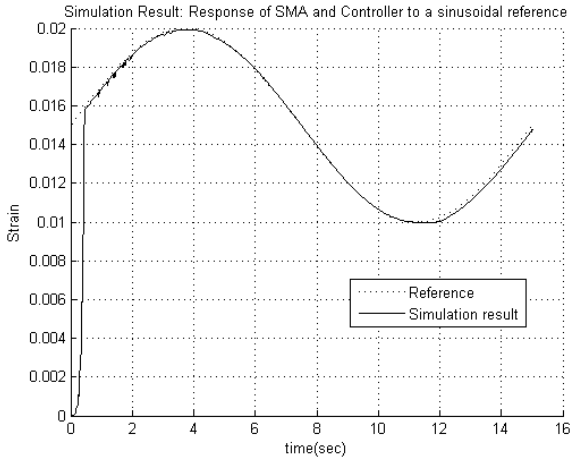

Fig. 7. Simulation result: Closed-loop SMA response to a sinusoidal input

$$= \sqrt{1 - \left\| \begin{bmatrix} \tilde{N}_s & \tilde{M}_s \end{bmatrix} \right\|_H^2} < 1 \tag{16}$$

where $\tilde{M}_s$ and $\tilde{N}_s$ define the normalized coprime factors of G_s. An $\epsilon \leq \epsilon_{max}$ is selected to form a stabilizing controller K_∞, which satisfies:

$$\left\| \begin{bmatrix} I \\ K_\infty \end{bmatrix} (I + G_s K_\infty)^{-1} \tilde{M}_s^{-1} \right\|_\infty \leq \epsilon^{-1} \doteq \gamma \tag{17}$$

The final feedback controller K is obtained as the product of the precompensator W_1 and the H_∞ controller K_∞ i.e.

$$K = W_1 K_\infty \tag{18}$$

VI. Simulation and Experimental results for the Controller

The simulation of the robust controller and the SMA was done on MATLAB. The desired loop shape was chosen so that the gains are high at low frequencies where the model describes the SMA accurately and the gains roll off at -20dB beyond the corner frequency, thereby ensuring a low gain at high frequencies. The open loop-shaping transfer function was chosen to be:

$$G_d(s) = \frac{\omega_0}{s} \tag{19}$$

where ω_0 is the corner frequency. A stabilizing H_∞ controller was designed to shape the singular value plot of $G(j\omega)K(j\omega)$ to have a desired loop shape $G_d(j\omega)$ with accuracy γ such that:

$$|G(j\omega)K(j\omega)| \geq \frac{1}{\gamma}|G_d(j\omega)| \qquad for \quad \omega < \omega_0 \tag{20}$$

$$|G(j\omega)K(j\omega)| \leq \frac{1}{\gamma}|G_d(j\omega)| \qquad for \quad \omega > \omega_0 \tag{21}$$

The value of the corner frequency was chosen to be 1000.424 $rad.sec^{-1}$. The singular value plot of $G(j\omega).K(j\omega)$ is shown in Figure 4 and the closed loop plot in Figure 5. The simulation result for input consisting of step

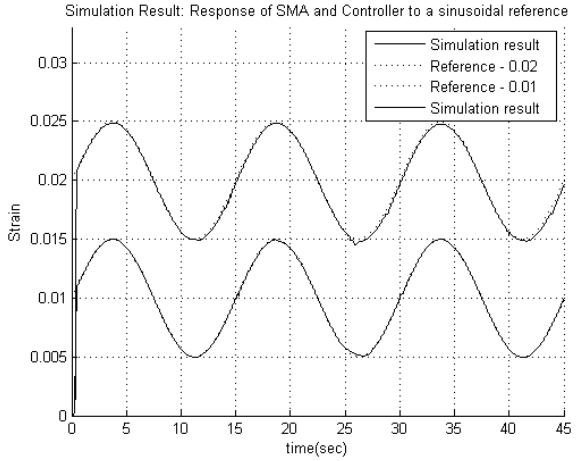

Fig. 8. Simulation result: Closed-loop SMA response to a sinusoidal input with different DC offset

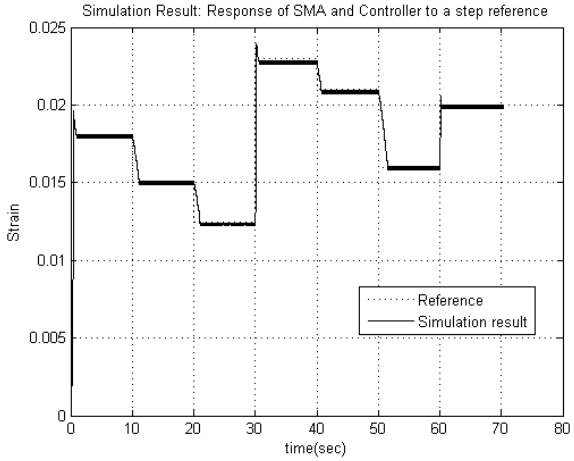

Fig. 10. Experimental result: Closed-loop SMA response to step changes

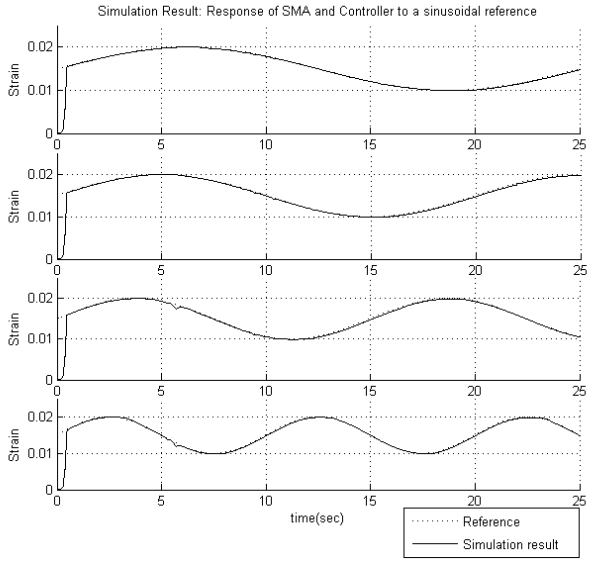

Fig. 9. Simulation result: Closed-loop SMA response to a sinusoidal input with different frequencies

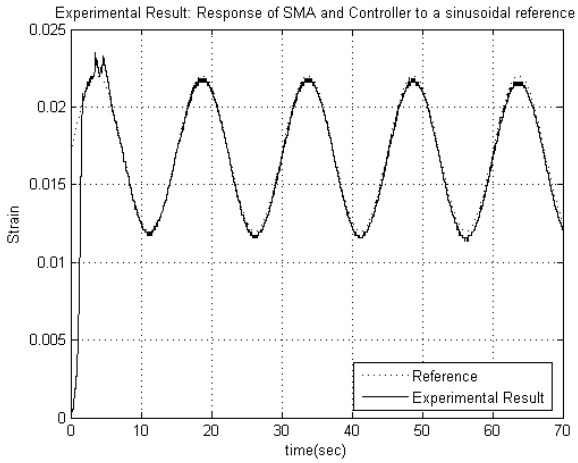

Fig. 11. Experimental result: Closed-loop SMA response to a sinusoidal input

changes is shown in Figure 6 and for a sinusoidal input is shown in Figure 7.

The performance of the controller was checked for the entire operating region by varying the DC offset of the sinusoidal reference, as shown in Figure 8. The simulation results were also evaluated for different frequencies of the sinusoidal inputs, as shown in Figure 9.

The experimental verification of the controller was done on a 700MHz Windows based PC at a sampling rate of about 100Hz. The response of the SMA to step changes is shown in Figure 10.

From the experimental results, it can be observed that the response time for heating is approximately 1.0 second and for cooling is 2.1 seconds for a 0.012" diameter SMA wire. The rate of heating and cooling are much higher for a thinner wire since the ratio of surface area to volume increases as the wire diameter is reduced, thereby increasing the rate of convectional cooling.

Figure 11 shows an excellent tracking of a sinusoidal reference trajectory by the SMA in closed loop. The DC offset of the sinusoidal reference input was also varied to obtain the experimental response of the SMA in the entire operating region, the results of which are shown in Figure 12. The frequency of the sinusoidal reference is also varied to check the performance of the controller and SMA. The results are shown in Figure 13.

VII. Conclusion

In this paper, we have shown the performance of an H_∞ loop-shaping controller for an SMA actuator. The simulation and experimental results show excellent tracking response for the SMA, thereby validating the model and the control scheme. This also clearly justifies the use of the model for describing the transformation between the Martensite

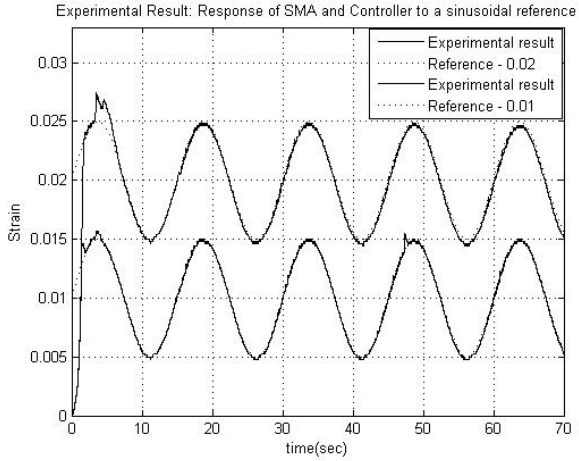

Fig. 12. Experimental result: Closed-loop SMA response to a sinusoidal input with different DC offset

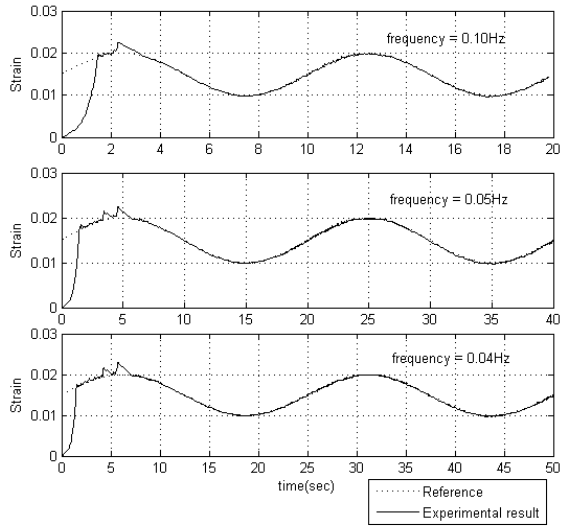

Fig. 13. Experimental result: Closed-loop SMA response to a sinusoidal input with different frequencies

and Austenite phases. The controller also has an ability to reject any uncertainties in the parameters of the model and unmodelled dynamics.

REFERENCES

[1] K. Glover and D. McFarlane, "Robust stabilisation of normalised coprime factor plant descriptions with H_∞ bounded uncertainty," *IEEE Transactions of Automatic Control*, vol. 34, pp. 821–830, August 1989.

[2] V. Le and M. Safonov, "Rational matrix GCD's and the design of squaring-down compensators - A state-space theory," *IEEE Transactions of Automatic Control*, vol. 37, pp. 384–392, March 1992.

[3] J. Jayender, R. Patel, S. Nikumb, and M. Ostojic, "Modelling and gain scheduled control of shape memory alloy," *submitted to the IEEE International Conference on Control Applications (CCA), Toronto, Canada, Aug.,2005*.

[4] K. Arai, S. Aramaki, and K. Yanagisawa, "Continuous system modeling of shape memory alloy (SMA) for control analysis," in *5th International Symposium on Micro Machine and Human Science*, 1994.

[5] S. Majima, K. Kodama, and T. Hasegawa, "Modeling of shape memory alloy actuator and tracking control system with the model," *IEEE Transactions on Control Systems Technology*, vol. 9, pp. 54–59, Jan. 2001.

[6] Y. Bernard, E. Mendes, and F. Bouillault, "Dynamic hysteresis modeling based on the Preisach model," *IEEE Transactions on Magnetics*, vol. 38, pp. 885–888, March 2002.

[7] M. Elahinia and H. Ashrafiuon, "Nonlinear control of a shape memory alloy actuated manipulator," *Journal of Vibration and Acoustics*, vol. 124, pp. 566–575, Oct. 2002.

[8] D. Grant and V. Hayward, "Variable structure control of shape memory alloy actuators," *IEEE Control Systems Magazine*, vol. 17, pp. 80–88, June 1997.

[9] D. Hughes and J. Wen, "Preisach modeling of piezoceramic and shape memory alloy hysteresis," *Proceedings of the 4th IEEE Conference on Control Applications*, pp. 1086–1091, 1995.

[10] K. Arai, S. Aramaki, and K. Yanagisawa, "Feedback linearization for SMA (shape memory alloy)," *Proceedings of the 34th SICE Annual Conference*, pp. 1383–1386, July 1995.

[11] M. Moallem and J. Lu, "Experimental results for nonlinear flexure control using shape memory alloy actuators," *International Conference on Robotics and Automation*, vol. 4, pp. 3653–3658, 2004.

[12] K. Zhou, J. C. Doyle, and K. Glover, *Robust and Optimal Control*. Prentice Hall, New Jersey, 1996.

[13] D. Chowdhury and D. Stauffer, *Principles of Equilibirium Statistical Mechanics*, 1st ed. Wiley-VCH, Weinheim, Germany, 2000.

[14] H. Khalil, *Nonlinear Systems*, 3rd ed. Prentice Hall, Englewood Cliff, NJ, New York, 2002.

Parameter	Value
Mass per unit length (m in $kg.m^{-1}$)	4.54e^{-4}
Specific heat capacity (c_p in $J.kg^{-1}.K^{-1}$)	320
Resistance per unit length (R in $\Omega.m^{-1}$)	8.0677
Youngs Modulus(Austenite) (D_a in $N.m^{-2}$)	75e^{9}
Youngs Modulus(Martensite) (D_m in $N.m^{-2}$)	28e^{9}
Thermal Expansion (θ_t in $N.m^{-2}.K^{-1}$)	-11e^{-6}
SMA initial strain(ϵ_0)	0.03090
Heat convection coefficient (h_0 in $J.m^{-2}.s^{-1}.K^{-1}$)	1.552
Heat convection coefficient (h_2 in $J.m^{-2}.s^{-1}.K^{-3}$)	4.060e^{-4}
Diameter of wire (in m)	304e^{-6}
Length of wire (in m)	0.24
Ambient temperature (T_a in ^oC)	20
Martensite to Austenite transformation temperature (T_{fa} in ^oC)	85
Austenite to Martensite transformation temperature (T_{fm} in ^oC)	42
Spread of temperature around T_{fa} (σ_a in ^oC)	6
Spread of temperature around T_{fm} (σ_m in ^oC)	4.5

TABLE I

PARAMETERS OF THE SMA